Electronic Noise Effects on Fundamental Lamb-Mode Acoustic Emission Signal Arrival Times Determined Using Wavelet Transform Results

Marvin A. Hamstad
University of Denver
Denver, CO 80208, USA

Abstract

Precise AE signal arrival times corresponding to known group velocities of energetic frequencies of the fundamental Lamb modes can be obtained from the arrival time of the peak wavelet transform (WT) magnitude at a particular frequency of interest. Since these arrival times are not determined from a fixed threshold they are not affected by dispersion, attenuation and source amplitude. Thus, at a particular frequency, they correspond to a single group velocity and lead to more accurate source location results than those obtained in traditional AE location calculations with threshold-based arrival times. Acoustic emission signals generated by finite element modeling (FEM) of the sources and signal propagation in a large aluminum plate (4.7 mm thick) provide essentially noise-free signals. In this research these FEM-based AE signals were combined with experimental wideband electronic noise to form noisy signals. Since the noise-free signal was available, the changes in the WT-based arrival times from noise-free to noise-altered signals could be quantitatively evaluated. Thus, an evaluation could be made that is not generally possible with experimental AE signals. Several signal-to-noise (S/N) ratios were examined in a statistical fashion for three important types of AE sources at a propagation distance of 180 mm. The WT-determined arrival times were obtained for the two different frequency-mode combinations (A_0 at 60 kHz and S_0 at 522 kHz) that represent the most energetic portions of the signals from multiple source types and depths in this thickness aluminum plate. Statistical calculations of linear source location were used to evaluate the errors in location accuracy caused by noise. Even at S/N ratios of 1 to 1, the location error was 2 % or less for a large majority of the cases.

Introduction

Previous publications [1, 2] have demonstrated the use of wavelet transform (WT) results to extract accurate acoustic emission (AE) signal arrival times. This technique determines arrival times that are independent of threshold, source amplitude, geometric-spreading-based attenuation, radiation direction and propagation-distance-based signal dispersion. Further, the arrival times correspond to a single group velocity (Lamb waves) of an energetic mode-frequency combination in the signal. A wideband AE signal database for several buried-dipole-type sources in a 4.7 mm thick aluminum plate was used for these demonstrations. This database was a subset of a broader database that was generated using a validated finite element modeling code [3-5]. The level of numerical noise in the AE signals obtained from the code is approximately three orders of magnitude less than the typical out-of-plane displacement signal levels.

Since real AE signals normally have significant electronic noise that is superimposed on the AE source-based signal, the purpose of the research reported here was to determine the effects of electronic (sensor/preamplifier-based) noise on the accuracy of WT-based arrival times. The finite element model (FEM) results are ideal for such a study since the noise-free signals are available. This situation is not the case with experimental AE signals. Further with experimental signals, the exact

location of the source is unknown, while for the FEM signals the precise locations of the source and pseudo sensor(s) are known.

Finite Element Modeled AE Signal Database

The signal database used in the research reported here has been described in previous publications [1, 2, 6, 7]. All the FEM signals were numerically processed with a 40 kHz (four-pole Butterworth) high-pass filter followed by resampling from 44.6 ns/point to 0.1 μs/point. The AE signals were based on a 1.5 μs source rise time, and they were examined out to 150 μs after the source operation time. This procedure avoids the plate edge reflections which appear well after the direct signals. The AE signal provides the out-of-plane top-surface displacement corresponding to a perfect point contact sensor located in the zero-degree propagation direction (in-plane, x-axis direction) at a distance of 180 mm from the source epicenter. Table 1 provides pertinent information on the buried-dipole-type AE sources used for a detailed examination of the effects of noise. The six cases described in the table were selected based upon the desire to include AE signal cases with the following features. First, an AE case having its primary signal energy (as evaluated by a WT) in the low frequency region of the fundamental anti-symmetric Lamb mode. Second, a case where the primary signal energy was in the high frequency portion of the fundamental symmetric Lamb mode. Third, a case where the primary-signal energy was approximately equally distributed between these two portions of the fundamental modes. And fourth, additional cases so each of the three source types was represented at two source depths. These source types were an in-plane dipole (aligned in the 0º direction), a microcrack initiation (with the primary dipole in the 0º direction), and a shear without a moment (about the in-plane y-axis). Previous research [1, 7] had identified the primary WT signal energy for this plate and these AE sources to be at the mode and frequency combinations of A_0 @ 60 kHz and S_0 @ 522 kHz. Table 1 specifies the dominant mode and frequency combination(s) for each case of source type and source depth. The table also provides the relevant average group velocities [1] and the ratio of the WT peak magnitudes (for each case) of these two mode and frequency combinations.

Wavelet Transform Information

The WT results were obtained using the AGU-Vallen Wavelet freeware [8] with the key parameter settings being: maximum frequency = 700 kHz; frequency resolution = 3 kHz and wavelet size = 600 samples. The Wavelet Time Range Setting for the number of samples (i.e., points) was 1500. Thus the signal was analyzed from the source operation time out to 150 μs. This allowed the full-direct-arrival signal to be transformed. The software automatically provides the arrival times of the peak WT magnitude at selected frequencies (really for a 3 kHz wide band in this research). The resolution of the arrival times was taken at 0.1 μs to correspond to the time resolution of the resampled FEM-based signals. The correspondence of the determined arrival times with the fundamental Lamb modes was facilitated by the software option to superimpose the group velocity curves on the WT results.

Description of Noise Signals and Creation of Modeled AE Signals plus Noise

To make the study of the effect of electronic noise as realistic as possible, the noise signals were obtained from a wideband high sensitivity conical sensor developed at NIST-Boulder [9, 10]. The noise signals were recorded at a preamplifier gain of 55 dB with the sensor coupled only to air and protected by soft foam from any

airborne signals. A total of ten noise signals was available. Each signal had been digitized by a 12-bit waveform recorder with a sampling interval of 0.1 μs/point corresponding to the resampled FEM signals. Each signal was 16384 points in length, which resulted in the ten signals representing a total of 16.384 ms of noise. A typical time domain and Fast Fourier Transform (FFT) from one of these ten signals is shown in figure 1. The slightly smoothed FFT was calculated after the signals had been numerically bandpass filtered (six-pole Butterworth) from 40 kHz to 1.2 MHz. This filter was used to make all the noise signals more representative of the frequency range of the FEM modeled signals. After modifying the noise signal amplitudes (so they were less than the FEM signal amplitudes) and changing the units to picometers, the signals were examined to determine their consistency. First, the peak magnitudes for the 10 noise signals were determined. The mean peak magnitude was found to be 0.63 pm with a dispersion of 10 % and a range of 0.54 to 0.73 pm. Thus the different noise signals were considered to be relatively uniform in their peak signal magnitudes.

Figure 2 shows the WT result of a 819.2 μs portion of a typical noise signal. Figure 3 demonstrates typical plots of the noise WT magnitude versus time at each of the two key frequencies. It is clear from this figure that the WT magnitude versus time varies over a wide range for each of the two key frequencies. The figure also shows the number of fluctuations of the WT magnitudes increases with increasing frequency (likely a characteristic of the WT used in this research). Further, the WT magnitude variations in figure 3 indicate, when noise is added to the FEM-generated AE signals the WT peak magnitudes of the signal plus noise (S+N) could experience noise-induced modifications. Since, for real-world AE signals, the amplitudes of the WTs of the underlying noise signal at the times of mode arrivals would be a random and unpredictable condition, a statistical study of noise effects on arrival times was necessary.

To form a suitable noise database for a statistical study a total of 50 different noise segments, each nominally 160 μs in length, was extracted from the modified database of ten noise signals. A S+N database was then constructed for the selected FEM cases (source type and depth) of interest. For each case the same 50 noise signals were added to the FEM-based (noise free) AE signal to form a database of 50 S+N signals. Before adding the noise signals they were multiplied by a factor to obtain a certain S/N ratio. This S/N ratio was based on the peak amplitude of each noise-free FEM signal and the mean peak amplitude (0.63 pm) representative of all the noise signals. The 50 S+N signals were called a “set” of S+N signals for a given FEM signal case. In order to be able to directly track the effects of different S/N ratios applied to the same FEM-based noise-free signals, the same sequence of noise signals (multiplied by a different factor to create a different S/N ratio) was added respectively to the noise-free signal to form each “set” of S+N signals. WTs of the S+N signals were then carried out for each case for the different S/N ratios, and the appropriate arrival times were obtained. Figure 4 shows examples of the S+N signals for case reference 2793 at four different S/N ratios.

Effects of Electronic Noise on WT-Determined Signal plus Noise Arrival Times

For each case (AE source type, source depth and S/N ratio) a total of 50 arrival times, at the mode and frequency combination(s) (shown in table 1), was obtained from the WT results. The 50 arrival times represent the effect of the random variation in the noise. Table 2 shows a statistical characterization of the arrival times as a function of the S/N ratio for one source type and depth. The table provides the

average arrival time, maximum time, minimum time and the standard deviation as well as the no-noise arrival time. Even at a 1 to 1 S/N ratio, the maximum and minimum times of 80.7 µs and 73.8 µs are not large deviations from the no-noise value of 78.2 µs. To justify the conclusion that these maximum and minimum times are not large, a threshold-based determination of possible arrival times was made for the relevant no-noise signal. Since the threshold method depends on the actual threshold used, a range of thresholds was used (equivalent to varying AE signal amplitudes with a fixed threshold). The range of arrival times determined was from 32.9 µs to 75.2 µs. This range of 42.3 µs is clearly much larger than the WT-based range of 6.3 µs. Thus the threshold-based method would likely lead to significant location errors.

Table 3 shows the average and standard deviations for all the cases (listed in table 1) at two S/N ratios (1 to 2 and 1 to 1). Compared to the no-noise arrival times, the average values are quite close to the no-noise values, even at a S/N ratio of 1 to 2. At this S/N ratio, a typical threshold-based system would not even record a hit.

Further examination of the results in table 3 leads to the interesting observation that the standard deviations are the largest for reference case 9002. As can be seen in table 1, the FEM-based no-noise signal for this case exhibited significant energy at both key mode/frequency combinations. This observation implies that when the noise-free AE signal energy is significant in more than one mode, then errors in WT-based arrival times will be greater than when the signal energy is predominantly in a portion of a single mode. This conclusion is consistent with the fact that the S/N ratio was related to the time domain while the WT-based results come from a time and frequency domain.

Location Errors versus S/N Ratio

The statistical properties discussed above do not address the important issue raised by the potential for noise to alter WT-based signal arrival times. The central issue concerns the effect of arrival time errors on the accuracy of the calculated AE source location. To address this question, a decision was made to focus on linear location. This choice was based on a desire to remove any dependence of the location error-analysis results on the particular computational scheme used for two-dimensional location calculations. Figure 4 shows a schematic of the linear location geometry and the notation used in this paper. Straightforward manipulation of the governing equations leads to the following:

$$d_1 = \tfrac{1}{2} [d - c_g (t_2 - t_1)], \quad (1)$$

$$d_2 = \tfrac{1}{2} [d + c_g (t_2 - t_1)], \quad (2)$$

$$d = d_1 + d_2, \quad (3)$$

where c_g is the appropriate group velocity, d is the sensor spacing, d_1 is the distance from the first hit sensor to the source location, d_2 is the distance from the second hit sensor. The values t_1 and t_2 are the respective arrival times. To allow the analysis to focus directly on arrival time errors due to the addition of noise, it was decided to consider geometry where the source was equally spaced between the two sensors (i.e., 180 mm from the source to each sensor). With this approach, when two different S+N signals (associated with the same no-noise case) are used to calculate a location, the location error will be directly due to noise-altered arrival times. When noise is present, equations (1) and (2) can be rewritten (with italics to denote the values when noise is present) as:

$$d_1 = \tfrac{1}{2} [d - c_g (\pm e)] \quad (4)$$

$$d_2 = ½ [d + c_g (\pm e)], \qquad (5)$$

where $e = |t_1 - t_2| > 0$ is the arrival time-difference error. On an absolute value basis the percent location errors in d_1 and d_2 values are equal, and this error is given by:

$$\% \text{ error} = [(c_g \cdot e) / d] \, 100. \qquad (6)$$

To form databases of delta time differences for each case (source type, depth and S/N ratio) the 50 arrival times obtained from each "set" were used in the following fashion. The absolute value differences of the first arrival time and each of the subsequent 49 values was determined. Then the absolute value differences of the second arrival time and each of the subsequent 48 values was determined. This process was continued in a similar fashion so that a total of 1225 arrival time differences were obtained for each case. These differences correspond to the *e* values in equation (6). Then using equation (6), the location errors were determined for each of the 1225 arrival time differences. Figure 6 shows as a function of the S/N ratio, the percentage of the 1225 trials for each case when the location error was 2 % or less based upon the sensor spacing (360 mm). In addition, figure 7 illustrates the maximum location error found in the 1225 trials for each case as a function of the S/N ratios. The data illustrated in figure 6 demonstrates that even with a S/N ratio of 1 to 1, at least 73% of the 1225 location calculations for each case resulted in a location error that was 2% or less. And figure 7 shows the maximum location error for the 1225 location calculations for each case was 13% or less. To appreciate these results, it should be pointed out that a typical fixed-threshold AE system would not even trigger on any of these signals because the required low threshold would trigger on multiple noise spikes.

At a 2 to 1 S/N ratio, figure 6 shows that at least 99% of the 1225 location calculations for each case would have location errors of 2% or less. And figure 7 shows the maximum location errors would be 2.4% or less. With a 2 to 1 S/N ratio, a fixed threshold AE system would likely trigger on real AE signals instead of noise spikes. And for a source equidistant between the sensors, the location errors would not be great. The reason is that the factors of geometric attenuation, dispersion, and variations in source amplitude would be the same for the signal at both sensors. But for a fixed threshold system, when the source is not equidistant from all the sensors, the above three factors would typically result in relatively large location errors compared to the 2% location error limit used in this research. On the other hand, the WT-based determination of arrival times would not be affected by the above three factors.

Finally, in the case of an AE source type and source depth that generates a signal with significant energy in portions of more than one fundamental mode, figures 6 and 7 show that the errors are greater at the S/N ratios of 1 to 2 and 1 to 1, for this type of source signal, as compared to cases where most of the AE energy is located in a portion of a single fundamental mode.

Conclusions

These conclusions are based on the following key conditions: a 4.7 mm thick large aluminum plate with a nominal wave propagation distance of 180 mm, the use of a particular WT; electronic noise from a particular wideband sensor/preamplifier; noise-free signals from finite element modeling that simulates perfect point contact

sensors; and the particular six cases of source types and source depths examined in detail.

- Due to random-noise-signal variations as a function of time, a statistical study of noise induced errors was necessary.
- At a S/N ratio of 2 to 1, the location error was 2% or less for at least 99% of the trials considering all the cases.
- Even at a S/N ratio of 1 to 1, the location error was 2% or less for at least 73% of the trials considering all the cases.
- At the lower S/N ratios of 1 to 2 and 1 to 1, the location and arrival time errors were greater if the combination of source type and source depth resulted in a signal with about equal energy in portions of both fundamental modes. This behavior was in contrast to smaller errors in cases where the signal energy was concentrated in a portion of a single mode.
- The errors in location with a fixed threshold are expected to be significantly greater since the arrival times generated will correspond to different group velocities due to the factors of geometric attenuation, dispersion, and source amplitude. These factors do not have a significant impact on the arrival time determined with the WT-based approach.

References

1. Hamstad, M. A., K. S. Downs and A. O'Gallagher "Practical Aspects of Acoustic Emission Source Location by a Wavelet Transform," Journal of Acoustic Emission, vol. 21, 2003, pp. 70-94, A1-A7
2. Hamstad, M. A., A. O'Gallagher and J. Gary, "Examination of the Application of a Wavelet Transform to Acoustic Emission Signals: Part 2. Source Location", Journal of Acoustic Emission, Vol. 20, 2002, pp. 62-81.
3. Gary, John and Marvin Hamstad, "On the Far-field Structure of Waves Generated by a Pencil Break on a Thin Plate," J. Acoustic Emission, Vol. 12, Nos. 3-4, 1994, pp. 157-170.
4. Prosser, W. H., M. A. Hamstad, J. Gary and A. O'Gallagher, "Reflections of AE Waves in Finite Plates: Finite Element Modeling and Experimental Measurements," Journal of Acoustic Emission, Vol. 17, No. 1-2, 1999, pp. 37-47.
5. Hamstad, M. A., A. O'Gallagher and J. Gary, "Modeling of Buried Acoustic Emission Monopole and Dipole Sources With a Finite Element Technique," Journal of Acoustic Emission, Vol. 17, No. 3-4, 1999, pp. 97-110.
6. Hamstad, M. A., A. O'Gallagher and J. Gary, "Examination of the Application of a Wavelet Transform to Acoustic Emission Signals: Part 1. Source Identification", Journal of Acoustic Emission, Vol. 20, 2002, pp. 39-61.
7. Downs, K. S., Hamstad, M. A., and A. O'Gallagher, "Wavelet Transform Signal Processing to Distinguish Different Acoustic Emission Sources," Journal of Acoustic Emission, vol. 21, 2003, pp. 52-69.
8. Vallen-Systeme GmbH, Münich, Germany, http://www.vallen.de/wavelet/index.html, 2001, software version R2002.0703.
9. Hamstad, M. A., and C. M. Fortunko, "Development of Practical Wideband High Fidelity Acoustic Emission Sensors," Nondestructive Evaluation of Aging Bridges and Highways, Steve Chase, Editor, Proc. SPIE 2456, Published by SPIE – The International Society for Optical Engineering, Bellingham, WA, 1995, pp. 281-288.
10. Hamstad, M. A., "Improved Signal-to-Noise Wideband Acoustic/Ultrasonic Contact Displacement Sensors for Wood and Polymers," Wood and Fiber Science, 29 (3), 1997, pp. 239-248.

Table 1 Description of the source cases examined [1]

Ref. no.	Source (depth/mm)	WT-based high intensity mode and freq., kHz	Average group velocity, mm/µs	Ratio WT peak magnitudes (A_0 @ 60)/S_0 @522
2793	In-plane dipole (1.723)	A_0 @ 60	2.5	1.3
9034	Shear (w/o moment)(0.783)	A_0 @ 60	2.5	5.6
9004	Microcrack initiation (1.41)	A_0 @ 60	2.5	4.1
9002	Microcrack initiation (2.037)	A_0 @ 60 S_0 @ 522	2.5 1.8	1 1
9030	Shear (w/o moment) (2.037)	S_0 @ 522	1.8	0.41
2791	In-plane dipole (2.35)	S_0 @ 522	1.8	0.001

Table 2 Statistical characterization of arrival times for the in-plane dipole source (reference number 2793) as a function of the S/N ratio

S/N Ratio	Avg., µs	Max., µs	Min., µs	Stan. dev., µs	Noise-free time, µs
4 to 1	78.2	78.4	77.7	0.1	78.2
2 to 1	77.9	78.8	75.6	0.8	78.2
1 to 1	77.4	80.7	73.8	1.6	78.2
0.5 to 1	81.2	113.7	73.6	8.2	78.2

Table 3 The average and standard deviation (50 samples) of the arrival times for the cases in table 1

Reference number and frequency, kHz	Avg. arriv. time and stan. dev., µs with S/N @ 1 to 2	Avg. arriv. time and stan. dev., µs with S/N @ 1 to 1	Noise-free arrival time, µs
2793 (60)	81.2 (8.2)	77.4 (1.6)	78.2
9034 (60)	77.4 (2.2)	77.5 (1.1)	77.9
9004 (60)	77.4 (1.9)	77.6 (1)	78
9002 (60)	78.4 (13)	77.5 (1.9)	78
9002 (522)	87.7 (28)	98.1 (4.2)	98.2
9030 (522)	94.2 (15)	98.1 (1.6)	98
2791 (522)	92.6 (17)	98.7 (1.6)	98

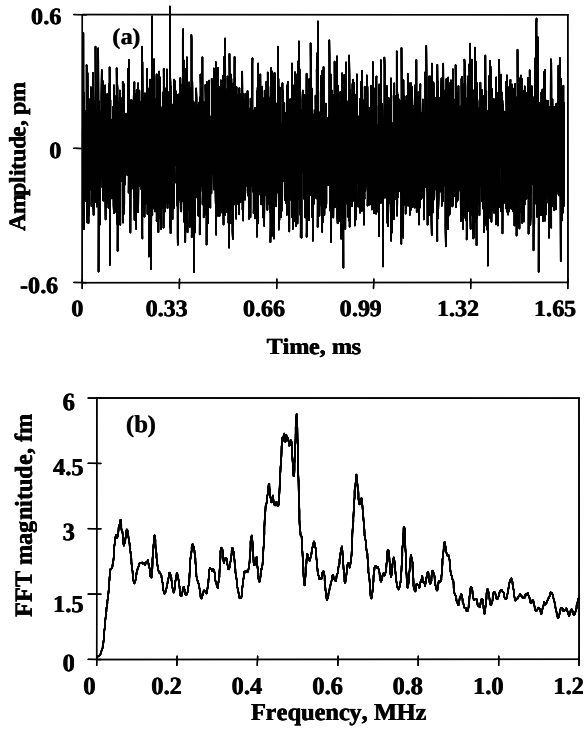

Figure 1 Time domain (a) and FFT (b) of a typical noise signal (after a gain of 55 dB) of 16384 points at 0.1 µs/point

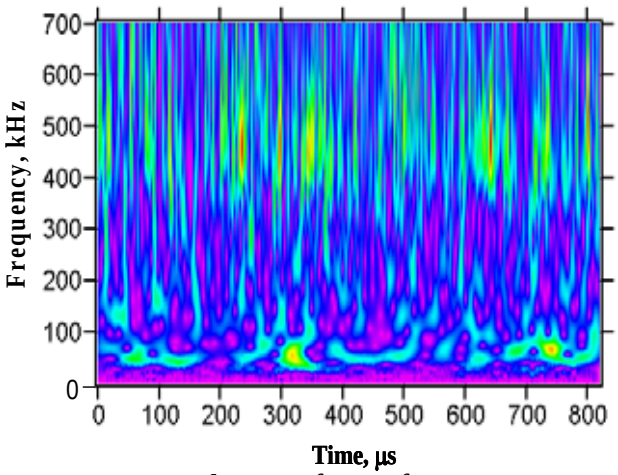

Figure 2 Wavelet transform of a 819.2 µs portion of a typical noise signal. Color or contrast shows WT intensity

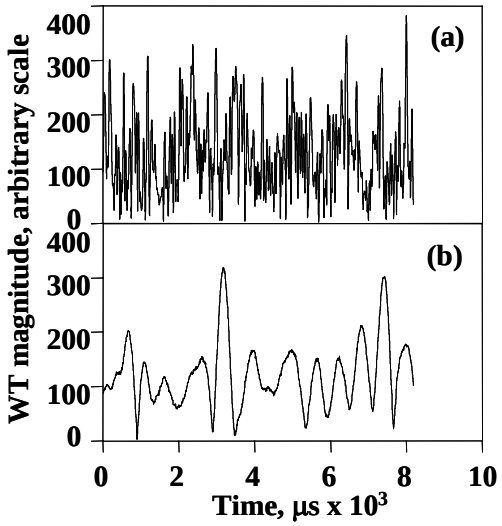

Figure 3 Magnitude of wavelet transform at (a) 522 kHz and (b) at 60 kHz versus time for a typical 819.2 µs noise signal

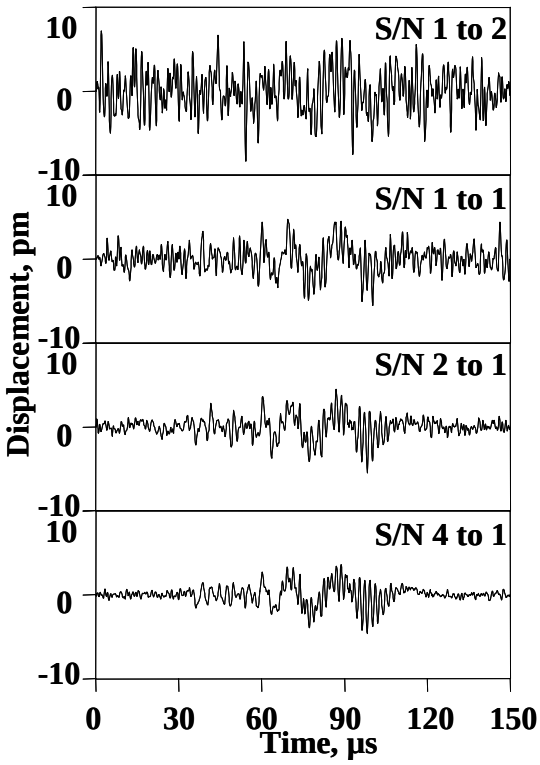

Figure 4 Typical examples of S+N signals for case reference 2793 at four different S/N ratios

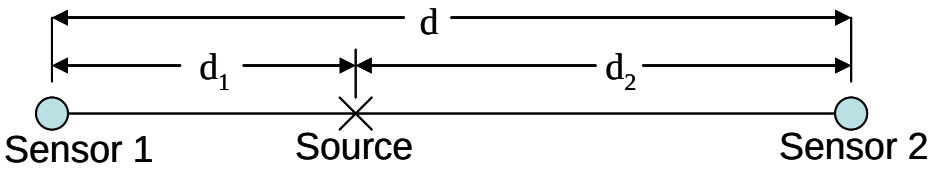

Figure 5 Geometry for linear location equations

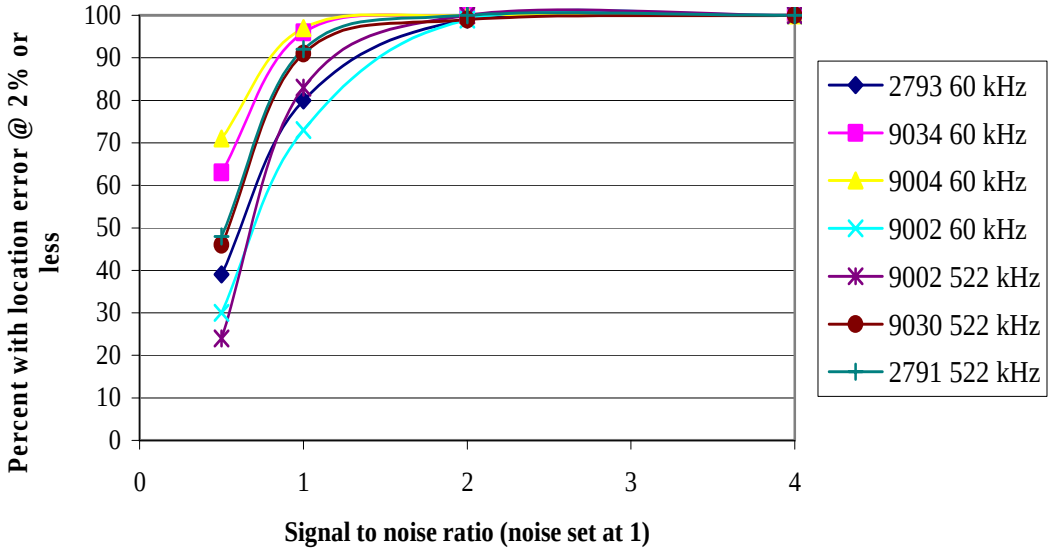

Figure 6 Percentage of the 1225 calculated locations with an error of 2% or less as a function of the S/N ratio for all cases (source type and depth)

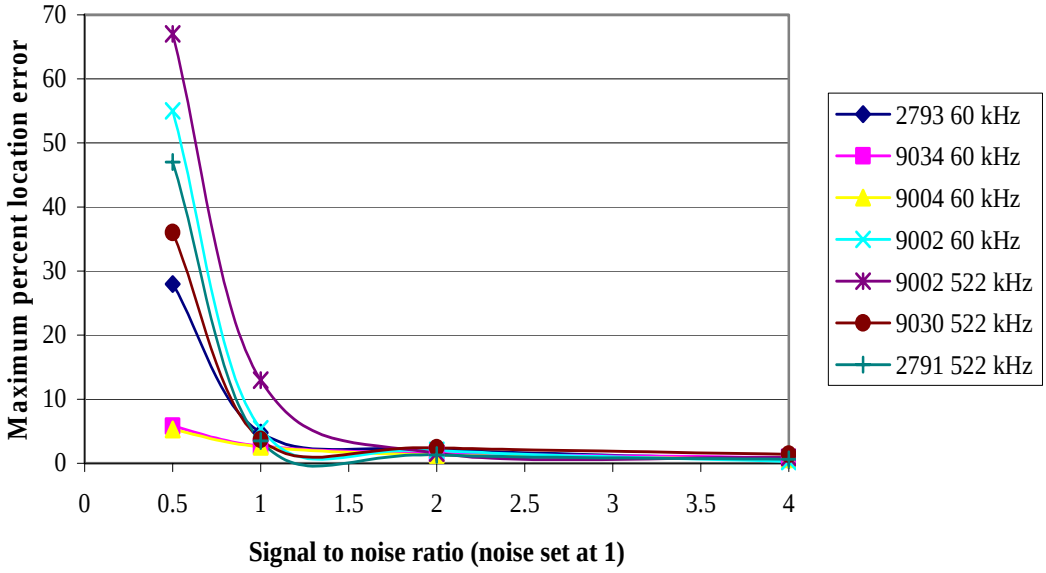

Figure 7 Maximum location error for the 1225 calculated locations for all cases as a function of the S/N ratio